LEVEL

NAVAL POSTGRADUATE SCHOOL
Monterey, California

THESIS

LABORATORY STUDY OF SOUND PROPAGATION INTO A
FAST BOTTOM MEDIUM,

by

James Arthur Bradshaw

June 1981

Thesis Advisor: James V. Sanders
Co-Advisor: Robert H. Bourke

Approved for public release; distribution unlimited

81 9 28 038

REPORT DOCUMENTATION PAGE	READ INSTRUCTIONS BEFORE COMPLETING FORM

1. REPORT NUMBER	2. GOVT ACCESSION NO. AD-A104 596	3. RECIPIENT'S CATALOG NUMBER

4. TITLE (and Subtitle)	5. TYPE OF REPORT & PERIOD COVERED
Laboratory Study of Sound Propagation into a Fast Bottom Medium	Master's/Meteorology and Oceanography (June 1981)
	6. PERFORMING ORG. REPORT NUMBER

7. AUTHOR(s)	8. CONTRACT OR GRANT NUMBER(s)
James Arthur Bradshaw	

9. PERFORMING ORGANIZATION NAME AND ADDRESS	10. PROGRAM ELEMENT, PROJECT, TASK AREA & WORK UNIT NUMBERS
Naval Postgraduate School Monterey, California 93940	

11. CONTROLLING OFFICE NAME AND ADDRESS	12. REPORT DATE
Naval Postgraduate School Monterey, California 93940	June 1981
	13. NUMBER OF PAGES 60

14. MONITORING AGENCY NAME & ADDRESS(if different from Controlling Office)	15. SECURITY CLASS. (of this report)
	Unclassified
	15a. DECLASSIFICATION/DOWNGRADING SCHEDULE

16. DISTRIBUTION STATEMENT (of this Report)

Approved for public release; distribution unlimited

17. DISTRIBUTION STATEMENT (of the abstract entered in Block 20, if different from Report)

18. SUPPLEMENTARY NOTES

19. KEY WORDS (Continue on reverse side if necessary and identify by block number)

fast bottom
acoustic reflection
attenuation
sound speed
sand

20. ABSTRACT (Continue on reverse side if necessary and identify by block number)

An experimental study was performed to determine the feasibility of a laboratory experiment to test an existing theoretical model describing sound propagation into a fast bottom underlying a wedge shaped medium. Sand under fresh water was found to satisfy the constraints of the theoretical model and to simulate the continental shelf. In a laboratory experiment, accuracy of density, sound speeds, and attenuation was shown to be sufficient to allow quantitative comparison to the predictions of the beam angle.

DD FORM 1473 EDITION OF 1 NOV 65 IS OBSOLETE
1 JAN 73
(Page 1)   S/N 0102-014-6601 |

1

Laboratory Study of Sound Propagation
into a Fast Bottom Medium

by

James Arthur Bradshaw
Lieutenant, United States Navy
B.S., Humboldt State College, 1971

Submitted in partial fulfillment of the
requirements for the degree of

MASTER OF SCIENCE IN METEOROLOGY AND OCEANOGRAPHY

from the

NAVAL POSTGRADUATE SCHOOL
June 1981

AUTHOR: _____

APPROVED BY: _____
                                          Thesis Advisor

_____
                                          Co-Advisor

_____
                      Chairman, Department of Oceanography

_____
                      Dean of Science and Engineering

2

ABSTRACT

An experimental study was performed to determine the feasibility of a laboratory experiment to test an existing theoretical model describing sound propagation into a fast bottom underlying a wedge shaped medium. Sand under fresh water was found to satisfy the constraints of the theoretical model and to simulate the continental shelf. In a laboratory experiment, accuracy of density, sound speeds, and attenuation was shown to be sufficient to allow quantitative comparison to the predictions of the beam angle.

TABLE OF CONTENTS

LIST OF FIGURES

LIST OF TABLES

I. INTRODUCTION

The behavior of radiation in a wedge-shaped medium overlying a fast-
bottom medium has been investigated both theoretically and experimentally
with both optical and acoustic sources. For example, in 1971 Tien and
Martin [Ref. 1] examined the behavior of a laser beam coupled into a thin,
tapered, dielectric film deposited on a substrate with a higher refrac-
tive index. As the light propagated toward the apex of the wedge shaped
film, perfect reflection was observed until the changing angle of inci-
dence decreased below the critical angle, then the light was converted
into radiation in the substrate.

An acoustic analog to the above optical study was performed by
Kuznetzov [Ref. 2] in 1973. Kuznetzov developed a normal mode theory
for sound propagation in both a wedge and underlying half-space substrate,
where the substrate sound speed was faster than that of the wedge.
Kuznetzov concluded that:

1. Sound traveling toward the wedge apex would be totall reflected
until the angle of incidence decreased to the limiting angle of total
reflection.

2. Any sound incident at less than the limiting angle of total re-
flection would be completely refracted into the underlying half-space.
This total refraction would occur along the wedge/half-space boundary
from the wedge apex to the point where the limiting angle was first
achieved.

3. Acoustic energy in the half-space would be columnated into a
well-defined beam. The beam's maximum pressure would occur at an angle

8

of depression (measured from the plane of the wedge/half-space interface) that would lie between β and 2β, where β is the wedge angle. Kuznetzov performed a series of experiments that supported his theory.

The formation of a well-defined beam within the substrate (for the optical case) was subsequently demonstrated by Tien, Smolinsky and Martin [Ref. 3]. Reference 3 also presented two theoretical results: (1) ray-optics predicted refraction into the substrate beyond the cutoff distance (the point at which the critical angle was reached) and (2) theory predicted refraction into the substrate before the cutoff distance.

A similar well-defined beam was predicted and observed by Sigelman, et al. [Ref. 4] in a water-aluminum system. Maximum pressure occurred at 11 degrees below the water-aluminum interface when the wedge angle was 1.3 degrees. This was well outside the range predicted by Kuznetzov. The observed beam was broader than predicted.

In 1980, Bradshaw [Ref. 5] extended a computer model first developed by Kawamura and Ioannou [Ref. 6] to describe the behavior of sound in a fast bottom underlying a wedge shaped medium. The model predicted the formation of well-defined beams in the bottom, and predicted the effect of attenuation in the bottom on the beam. A comparison of the predictions of this model with the experimental data of Netzorg [Ref. 7] gave qualitative agreement, but since the experiment did not match all model constraints, quantitative comparison was impossible. It is the purpose of this laboratory analysis to determine if a laboratory experiment that fulfills the constraints of the model can be designed. If at all possible, it is further desired to model the continental shelf in the design of the experiment.

II. CONSTRAINTS

The general design of the proposed experiment is illustrated in Figure 1. Constraints will be imposed by both the theoretical model and the measurements.

A. MODEL CONSTRAINTS

The Bradshaw model [Ref. 5] requires that the sound speed in the bottom exceed that in the overlying wedge. Physical parameters required to be known are the density and sound speed of the two media, the slope of the wedge, and the attenuation of the substrate medium. A further constraint, dependent on the substrate sound speed, will be discussed in detail later. This model assumes planar waves incident on the wedge-bottom interface.

B. OTHER CONSTRAINTS

Since it was desired to model a real-world environment, specifically the continental shelf, a laboratory set-up consisting of fresh water over sand was an obvious first choice. The sound speed of fresh water was expected to be about 1481 m/s [Ref. 8] and the speed in sand about 1700 m/s [Ref. 9]. Thus, the requirement of a faster bottom medium would be readily fulfilled.

A wedge of water would require a high frequency (i.e., greater than 100 kHz) to permit planar incident waves in a laboratory-sized experiment. If one hundred wavelengths are desired to ensure plane waves, at 100 kHz the source would need to be 1.5 m away from the wedge apex.

10

The use of a water/sand system would permit the hydrophone to be moved about in both media; the use of plaster to simulate rock, for example, would not. While it would also be necessary to maintain a flat slope of at least five degrees between the two media, a water-sand system was expected to be adequately stable. The smoothness of the slope is required by the model; the five degree slope encompasses the maximum for the continental shelf.
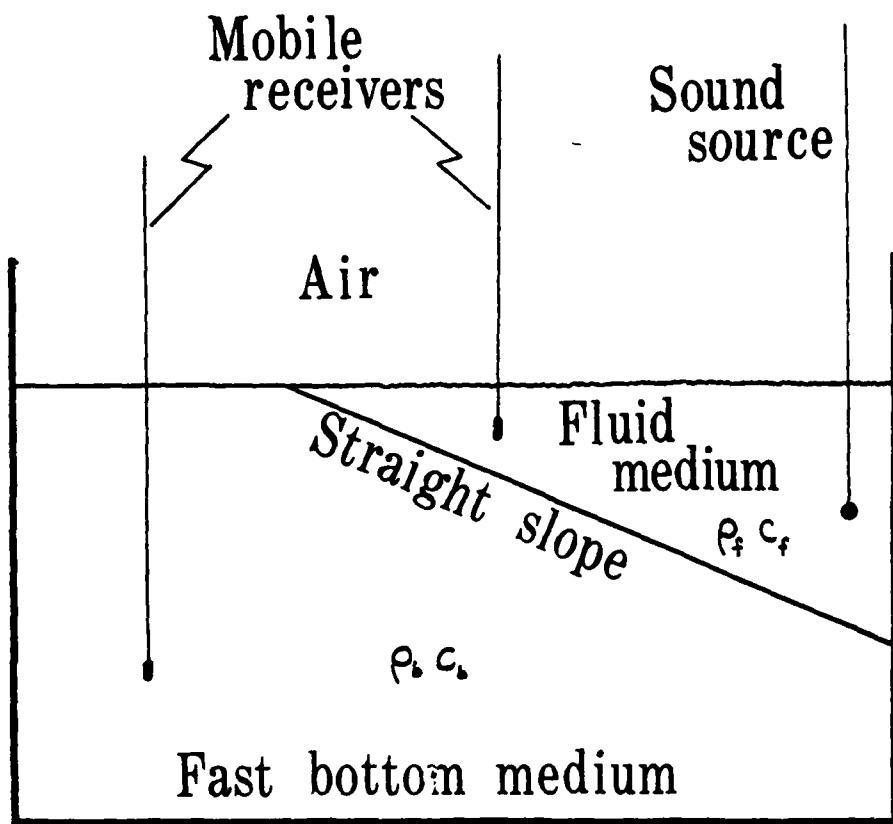
Figure 1. Model Geometry

III. EXPERIMENTAL DESIGN

A. MATERIAL SELECTED

Fresh (tap) water and #30 fine sand were the media used in the experiment. The grain size of #30 fine sand varies from 0.70 mm to 0.15 mm. It was readily demonstrated that the sand could maintain a slope as large as 25 degrees. To remove all air bubbles, the water/sand system was heated with immersion heaters. Bleach was added at a ratio of one-half gallon bleach to 70 gallons of water plus sand in order to control biologic growth.

B. VELOCITY MEASUREMENT TECHNIQUES

An excellent summary of methods for measuring sound speeds in rocks and minerals is given by Anderson and Liebermann [Ref. 10]. Specialized methods for use on small specimens, iron compounds, etc. or for high pressure and temperature systems were eliminated as inappropriate for the experiment being considered. Ultrasonic interferometry was also discarded despite its exceptional accuracy (0.01 to 0.04 percent) as it is best applied to nonporous samples and utilizes frequencies (10-60 MHz) that would cause unacceptable attenuation in the verification experiments. Resonance methods with appropriate frequencies and accuracies were undesirable as they are applicable to crystalline specimens only. Ultimately, pulse transmissions were selected as they best fit the necessary criteria. This method is applicable to either fluid or porous materials, acceptable over a frequency range of 50 kHz to 10 MHz, and accurate to within one to three percent.

13

1. Size Criteria

Steel-bound glass tanks measuring 70 cm square by 60 cm high were readily available. Length vs depth criteria, from Reference 10, require that the layer of sand on the tank bottom should not be less than 14 cm to avoid boundary reflection problems. To satisfy this constraint, a sand layer of 20 cm was chosen.

To avoid pulse dispersion, Reference 10 also suggested that the sand depth not be less than five wavelengths. Since the sound speed of the sand was expected to be 1700 m/s, and the frequency would be of the order of 100 kHz, five wavelengths would be 8.5 cm. A sand depth of 20 cm would also satisfy this restraint.

To avoid particulate scattering, the wavelength must be at least three times the grain size [Ref. 10]. Since the largest grain size in number 30 sand is 0.070 cm, a wavelength, equal to 1.7 cm, readily qualifies.

Since sound speed is not a function of frequency [Ref. 9], results from this laboratory analysis were expected to be applicable to frequencies used in the experiments.

2. Electronic Equipment

A schematic of the equipment configuration is shown in Figure 2. All components were off-the-shelf and readily available.

Output from a General Radio model 1310 oscillator with a frequency range of 2 Hz to 2 MHz was fed simultaneously into a frequency counter and a tone burst generator. The counter, a Hewlett-Packard 5233L, would read ±10 Hz at 100 kHz. The General Radio Type 396-A tone burst generator was used to generate either 8 or 16 cycle pulses. The

14

output passed through a Hewlett-Packard HP 467-A power amplifier before being fed to a transducer. The pulsed signal was also fed to the trigger input of a Tektronix type Rm-503 oscilloscope.

Three types of transducers were used as sources. The first was a homemade, mylar, broad-band transducer with a 3 cm by 9 cm active face. This source was quite directional at 100 kHz but proved to be difficult to move through the sand (for sound speed and attenuation measurements) and was not sufficiently powerful to generate usable signals in the sand (as would be required in model verification runs). The mylar transducer required by 150 V DC supply and polarizing network.

A second, smaller, homemade transducer was tried as a source. This transducer, a matrix of ceramic elements, has a 1 x 2 cm active face and was highly directional at 100 kHz. This transducer offered little improvement over the first.

Celesco Industries type LC10 hydrophones had been consistently used as receivers. The LC10 is a small (0.97 cm diameter by 2.87 cm long) cylinder, with a receiving range of 0.1 to 120,000 Hertz. The transducer is designed to be omnidirectional in a plane perpendicular to the axis of the cylinder with a tolerance of ± 1 dB at 100 kHz, and omnidirectional in a plane containing the axis of the cylinder with a tolerance of ± 2 dB at 25 Hz. The omnidirectional characteristic was not desirable for the source, as this would increase the number of possible reflected signals from the walls, water surface, etc., but the small size and higher signal strength were desirable. Geometry was used to isolate desired signals and will be described when appropriate.

15

Because the direct and reflected pulses arrived from different directions, use of LC10's as the source and receiver for attenuation measurements initially produced non-reproducible results. Directivity measurements in the plane perpendicular to the axis of the cylinder were made and the results are shown in Figs. 3 and 4. Subsequent measurements used LC10 number 2338 as a source and LC10 number 2319 as a receiver. The receiver was oriented to use the area about 50 degrees as the receiving face. The transducers were always arranged geometrically to use the radial plane.

The received signals were amplified 20 dB by a Hewlett-Packard HP-465A amplifier, then passed through a Spencer-Kennedy Laboratories, Inc. model 302 variable electronic filter (set at 60 kHz high pass) to eliminate low frequency mechanical noise present in the laboratory before being passed to the oscilloscope. The data of Fig. 5 demonstrates that spherical spreading (1/r) was observed for all LC10 source-receiver separations greater than 8.4 cm. All measurements were made under far-field conditions.
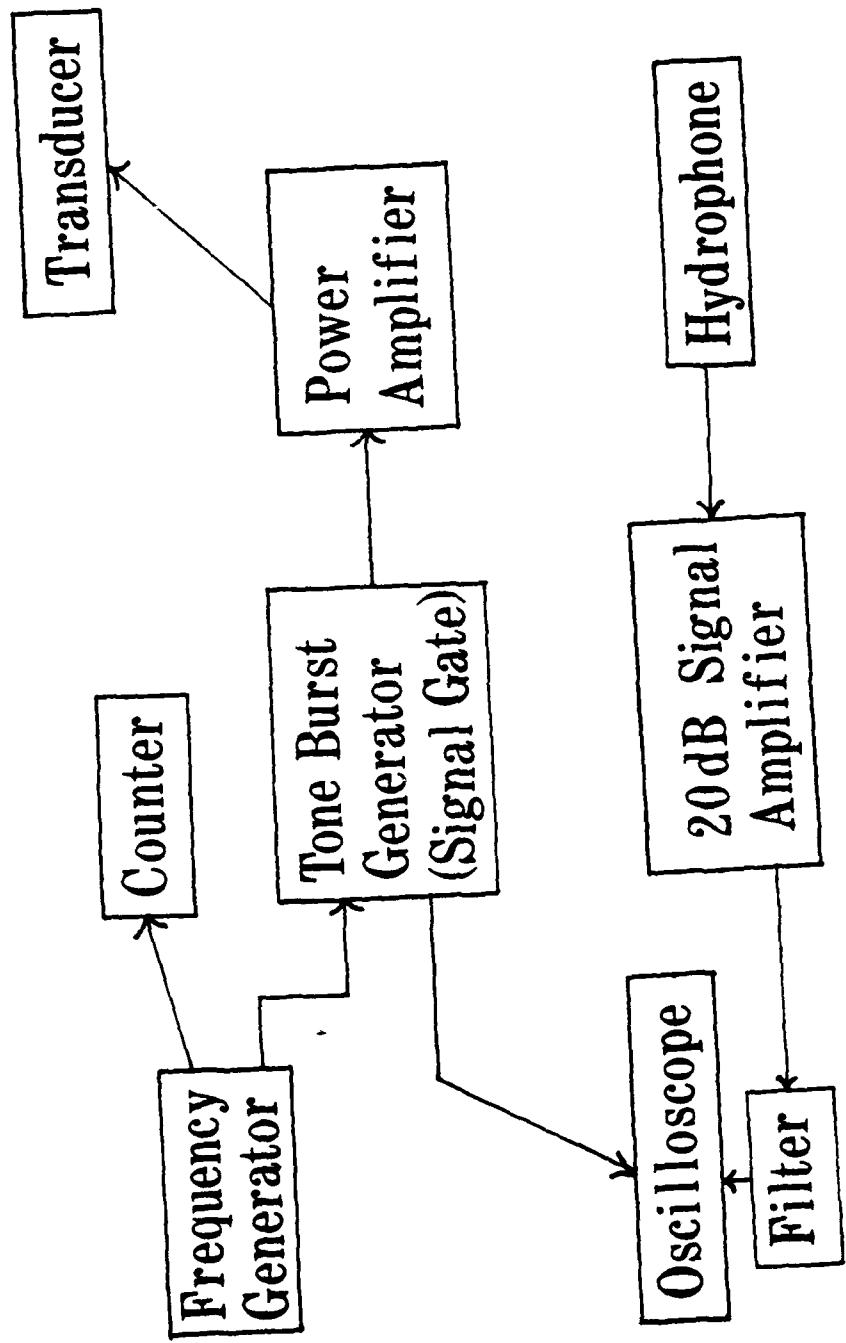
Figure 2. Electronic Equipment Schematic
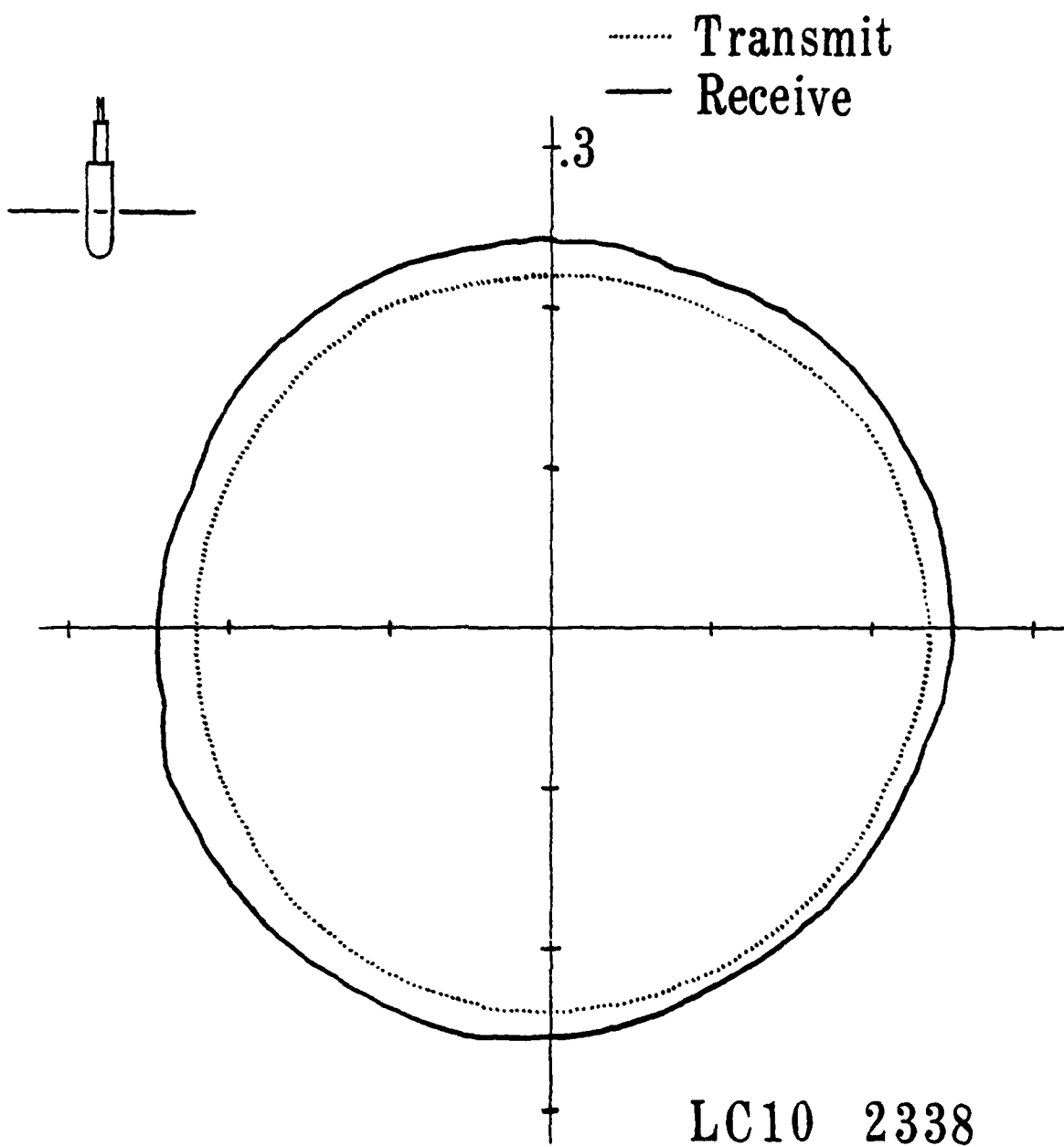
Figure 3. LC10 2338 Directivity Pattern
(units of volts)

18
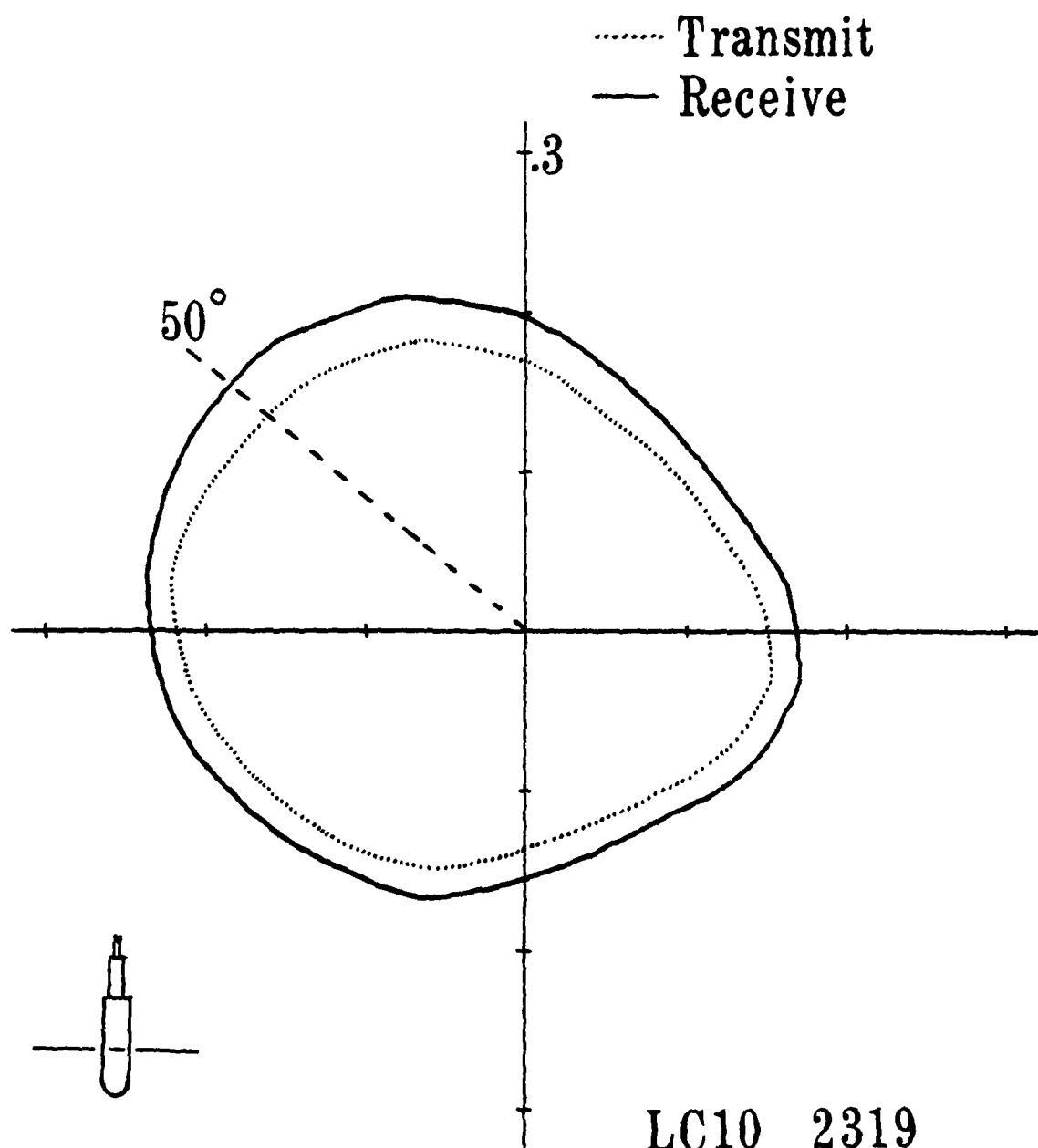
Figure 4.   LC10 2319 Directivity Pattern
(units of volts)

19
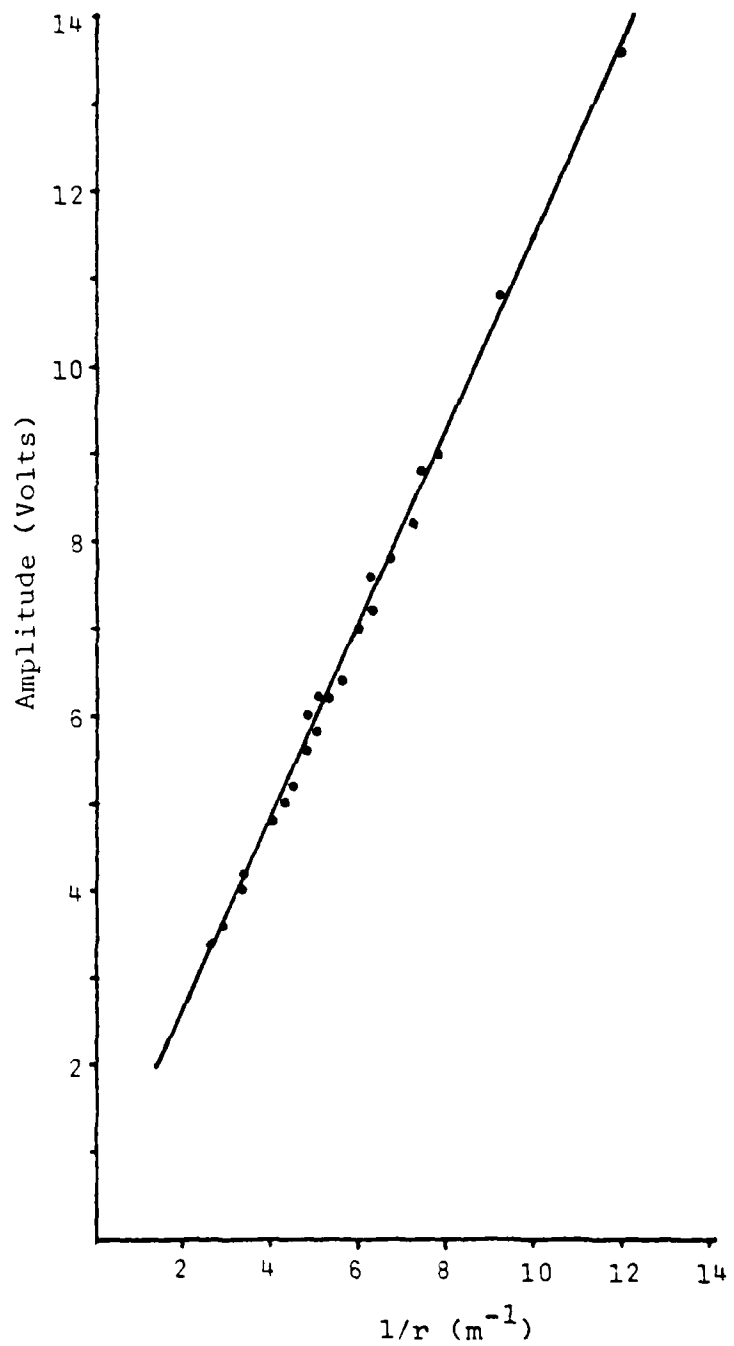
Figure 5.   1/r Spreading for LC10

20

IV. MEASURED DATA

For all of the following measurements, the sand layer in the tank was kept flat and horizontal, as only physical parameters were being determined and not wedge characteristics.

A. DENSITY

1. Water

According to Lange's "Handbook of Chemistry" [Ref. 11], the density of distilled water ranges from 0.99913 g/cm^3 at 15°C to 0.99707 g/cm^3 at 25°C. The expected density of room temperature water, to 3 significant figures, was therefore 1.00 g/cm^3. Measured volumes of the bleached water were periodically weighed, and the observed density was 1.00 g/cm^3, with no noted variation.

2. Sand

The density of water saturated sand was measured by partially filling a weighed 100 ml graduated cylinder with a water over sand mixture, observing the volume of each, and using a density of 1.00 g/cm^3 for the water to calculate the weight of the water volume. The density of the water saturated sand, for eight separate measurements, was 1.98±0.03 g/cm^3.

B. SOUND SPEED

1. Water

Three separate sets of sound speed in water measurements were made. The first involved the use of the mylar transducer as the source.

One LC10 was placed 20.1 cm away, and the second LC10 was moved along the straight line defined by the source and first receiver. The time of flight between the two receivers was measured. A simultaneous check for 1/r dependence confirmed these measurements were all in the far-field. The data are summarized in Table 1 of Appendix A. The average sound speed was 1454 m/s with an (N-1) variance of 33 m/s.

The second set of data utilized a reflected signal to increase the total path length. The mylar source was fixed, and the receiver, placed between the source and the wall, was moved along a perpendicular line between the source and the wall. The time of flight was the time difference between the arrival of the direct and reflected signals; the distance was twice the distance from the receiver to the wall. These results are summarized in Table 2 of Appendix A. The average speed was 1469 m/s, with a variance of 14.7 m/s.

In the third set of measurements, the distance over which the time of flight was measured was fixed. The LC10 source was suspended 11.0 cm from the tank wall, the second LC10, placed further from the wall than the source, was moved along the perpendicular formed by the wall and the source. As the receiver was moved, the distance difference between the direct path signal and the signal reflected from the wall remained a constant 22.0 cm. The time difference between the arrival of the two signals was recorded. Table 3 of Appendix A summarizes the results. The average speed was 1460 m/s, the variance was 19 m/s.

The data compared well with theory. From Kinsler and Frey [Ref. 8], the equation of sound for distilled water is given by

$$c_w = 1403 + 5t - 0.06t^2 + 0.0003t^3 \qquad (1)$$

22

where t is the temperature in degrees Celcius. A comparison of measured
and theoretical values is presented in Table VI-1. Note that direct
path results showed greater variation, but all results were within two
percent of expected values.

2. Sand

Five separate sets of sound speed measurements were made in the
sand; four in conjunction with attenuation data, and one to check for a
sound speed gradient. All three source transducers were used. For the
attenuation runs, the source was buried at a fixed depth, probing was
with an LC10 receiver inside a glass tube for the depth of maximum signal
amplitude. The glass tubes were necessary to prevent abrasive damage to
the receiver. The data are summarized in Tables 1 through 4 of Appendix
B.

The fifth set of data utilized the two LC10's fixed 30 cm apart.
The transducers were initially placed in water and sand was added to
progressively bury them. The entire process was carried out underwater,
so degassed, saturated sand was used. The data are summarized in Table
5 of Appendix B. Table IV-2 lists the resultant sound speeds.

a. Theoretical Sound Speed in Sand

Since a search of the literature revealed many theoretical
and experimental values for the speed of sound in sand under brine, but
not under fresh water, and since the values given were greater than
those observed in this experiment, the following analysis was performed
to derive a theoretical value for sound speed in sand under fresh water.

From Urick [Ref. 12], the density of a liquid-sediment
mixture is given by

23

Table IV-1. Measured vs Theoretical Sound Speed in Water

Measurement Method	$\bar{c}_w$ (m/s)	σ (m/s)	$\sigma / \bar{c}_w$	t (°C)	c_w (m/s)	$|\bar{c}_w - c_w|$ (m/s)	$\dfrac{|\bar{c}_w - c_w|}{c_w}$
Direct path	1454	33	2.2%	19.0	1478	24	1.6%
Reflected path, varied	1469	15	1.0%	20.0	1481	12	0.8%
Reflected path, distance fixed	1460	19	1.3%	18.3	1476	16	1.1%

$$\rho_{mix} = \gamma\rho_w + (1 - \gamma)\rho_s \qquad (2)$$

where ρ_{mix} = the density of the mixture,

γ = the porosity,

ρ_w = density of water,

and ρ_s = the density of individual sand grains.

From equation (2), using the measured value ρ_{mix} = 1.98 g/cm^3 and ρ_s = 2.69 g/cm^3 from Reference 9, gives γ = 0.42. Also from Reference 12, the speed of sound in the saturated sediment is given by

$$c_{mix} = \left[(\rho_w\gamma + \rho_s(1 - \gamma))(k_w\gamma + k_s(1 - \gamma))\right]^{-1/2} \qquad (3)$$

where k_w and k_s are the compressibility of the water and sand, respectively. Values for k_w and k_s were calculated from the relationships

$$c_w = (\rho_w k_w)^{-1/2} \qquad (4)$$

and

$$c_s = (\rho_s k_s)^{-1/2} \qquad (5)$$

Setting c_w = 1481 m/s [Ref. 8], and ρ_w = 1.0 g/cm^3, and solving for k_w yields

$$k_w = 4.56 \times 10^{-13} \text{ m sec}^2 \text{ g}^{-1} \qquad (6)$$

The sand in the experiment was composed of quartz particles. From Anderson and Lieberman [Ref. 10], page 360, c_s was set to 7000 m/s. Solving equation (5) yields

$$k_s = 7.59 \times 10^{-15} \text{ m sec}^2 \text{ g}^{-1} \qquad (7)$$

Substituting the above values in equation (3) and solving for c_{mix} yields an expected speed for sand under fresh water of 1605 m/s.

A comparison of the expected value with the sound speeds summarized in Table IV-2 shows close correlation with the value obtained

TABLE IV-2. Measured Sound Speeds in Sand

Measurement Method	Sound Speed (m/s)	(N-1) σ (m/s)
Variable distance	1579	58.6
Variable distance	1597	44.7
Variable distance	1434	71.9
Variable distance	1567	32.6
Fixed source/receiver	1613	0.0

using a fixed source-receiver distance (1613 m/s) but not close agreement with the majority of values obtained from measurements utilizing glass tubes. The use of glass tubes disturbs the medium, and the distance from source to receiver is not accurately measurable. Over the short distances used, a 0.5 cm error in the distance would lead to significant errors. Thus, the value obtained from the fixed source and receiver method is more likely accurate, and, not unexpectedly, shows closer agreement with the theoretical values.

   b. Sound Speed Gradient

      As illustrated in Fig. 6, Hamilton [Ref. 13] predicts a pronounced sound speed gradient in a fine sand sediment. A change in slope of 27 s^{-1} is specified at zero depth. Although the gradients were established for sand under brine, they are attributed to a decrease in sediment porosity with pressure, to temperature effects, and to pressure effects on the pore water, and would therefore be expected to be present in fresh water systems as well. Sound speed measurements tabulated in Table 5 of Appendix B were taken specifically to check for the presence of a gradient. None was found within the accuracy limitations of the method. For a sound speed of 1613 m/s, a 2% error (see Sec. III-A) would be 32 m/s and would mask a 27 m/s change. Even if a 27 m/s gradient were present, the resulting 62 m radius of curvature would not be sufficient to be detectable over the experimental ranges. The lack of a detectable gradient, although not mirroring actual continental shelf conditions, is consistent with the isovelocity substrate assumed in Bradshaw's model [Ref. 5].

27
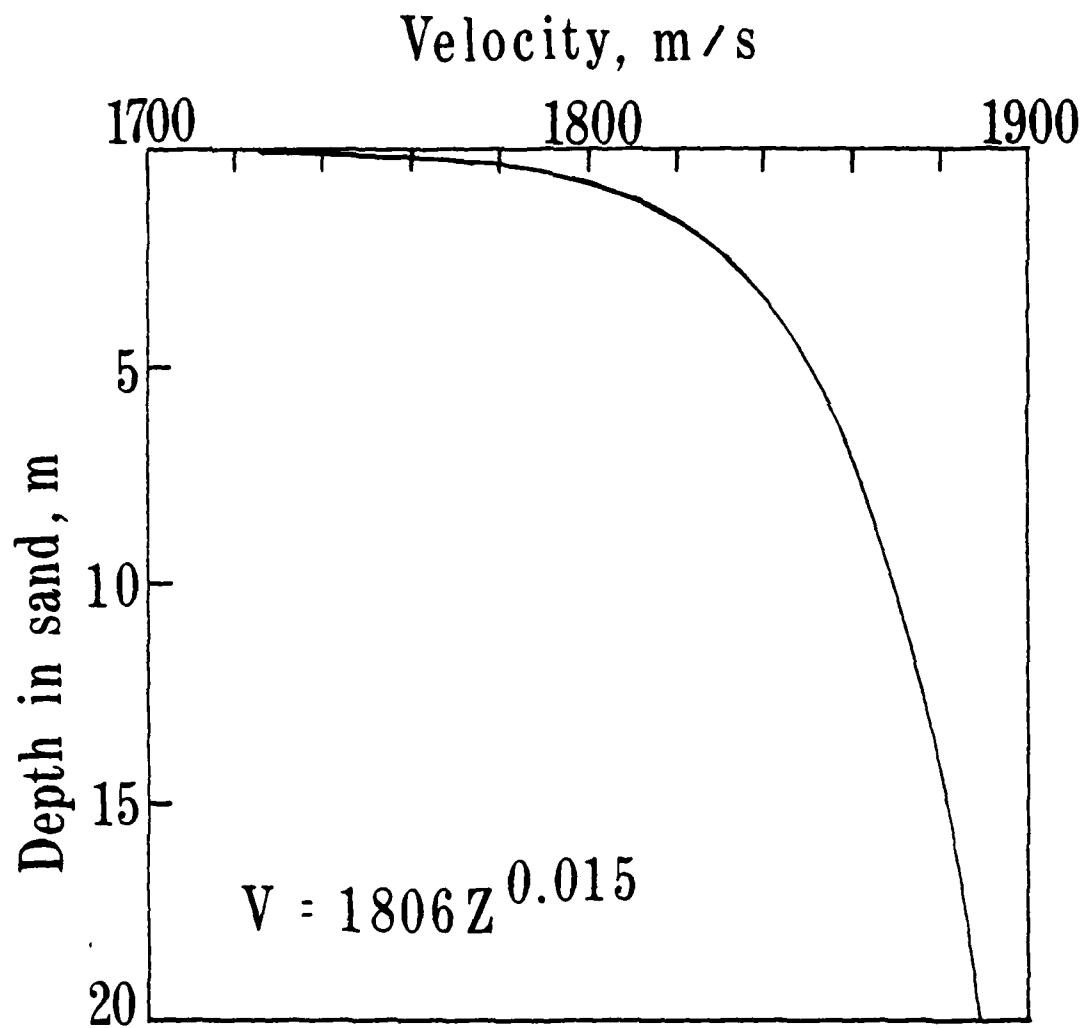
Figure 6. Sound Speed Gradient in Brine Saturated Sand (adapted from reference 13.)

C. ATTENUATION

1. Model Limitations

It was mentioned in Section II-A that a further constraint, to be defined once the substrate sound speed had been determined, must be fulfilled for verification of Bradshaw's model. This constraint is that the signal must propagate beyond a specific range determined as follows. The model uses a Green's function analysis to obtain the pressure and phase distribution of the sound in the bottom. To solve the appropriate Green's function, it was necessary to assume that

$$k_2 |\vec{r} - \vec{r}'| \gg 2\pi \tag{8}$$

where $k_2 = \omega/c_s$ is the wave number for the sound in the sand. Using the determined sound speed of 1613 m/s and assuming a frequency of 100 kHz, k_2 equals 389 m^{-1}. Thus, it is required that $|\vec{r} - \vec{r}'| \gg 0.016$ m

The quantity $|\vec{r} - \vec{r}'|$ is defined in Fig. 7. The quantity $\vec{r}'$ is the distance from the wedge apex to a point on the wedge-substrate boundary (integration in the model is carried out over $\vec{r}'$). The quantity $\vec{r}$ is the distance from a point along the wedge-substrate boundary, called X, to the field point. The distance X is the distance at which the critical angle is reached and where lowest mode transmission into the substrate begins. The distance is defined by

$$X = \frac{c_w}{4 \, f \, \sin\theta_c \, \sin\beta}; \tag{9}$$

$$\theta_c = \arccos (c_w/c_s) \tag{10}$$

where f is the frequency,

β is the wedge angle

c_w, c_s are the sound speeds in the wedge fluid and substrate, respectively,

29
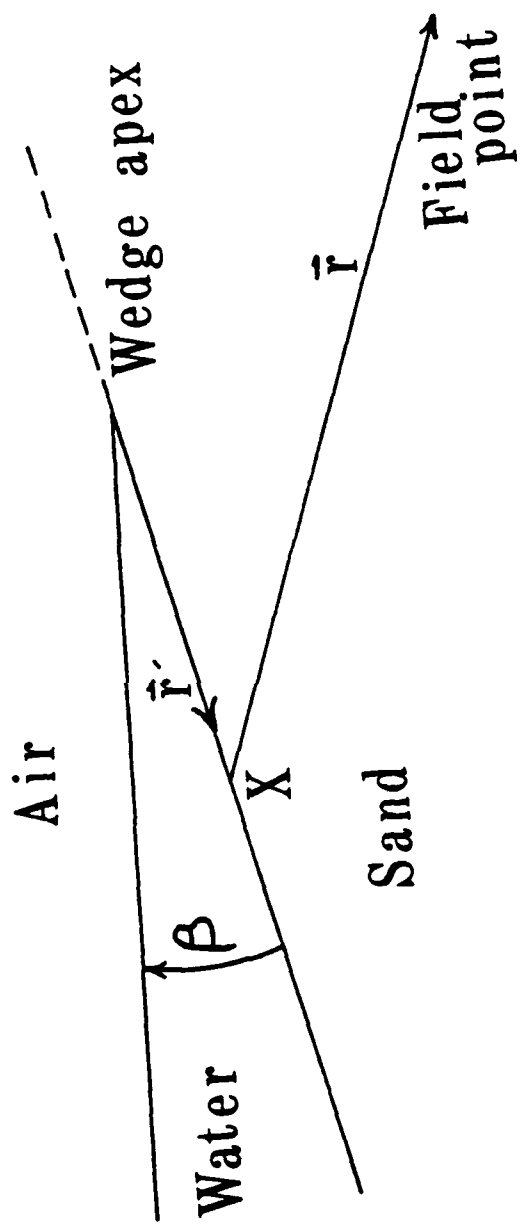
Figure 7. Geometry for the Wedge Model.

and θ_c is the critical angle.

For f = 100 kHz, a wedge angle of 3°, c_w = 1469 m/s and c_s = 1613 m/s, X would equal 0.17 m.

Typically, within the model, the integration limit is from nX to NX, where n = 0,1,2,..., N = 1,2,3,..., N>n. In the simplest case, the integration would be carried out from 0 to X. This places a constraint on $\vec{r}$, and thus on permitted attenuation.

Consider, as a minimum, a factor of 10 to satisfy the "much greater than" inequality; this would require $|\vec{r} - \vec{r}'|$ to be greater than 0.16 m. This implies mathematically that no measurements may be made at point $\vec{r}$ within a circle of radius 16 cm about the point $\vec{r}'$, and since $\vec{r}'$ can vary from 0.0 to 0.17 m, an area of "forbidden territory" is traced about the wedge apex and boundary surface. Thus, to test the model, since measurements must be made outside this area, the attenuation must not be so great that insufficient signal remains beyond the forbidden zone. (If "much greater than" were taken to be 100 times, measurements would have to be made over 1.6 m from the boundary).

2. Results

The methodology for collecting attenuation data was described in Section IV-B-2. The data were processed graphically. Taking the natural logarithm of the well-known equation

$$V = \frac{V_0}{r} e^{-\alpha r} \tag{11}$$

where V is the measured voltage,

V_0 is the source voltage,

r is the distance from the source,

and α is the attenuation,

31

the linear relation

$$\ln(Vr) = \ln(V_o) - \alpha r \qquad (12)$$

is obtained. Thus α, in nepers per meter, will be the slope of a graph of $\ln(Vr)$ vs r. Graphs of the four data sets of Appendix B are shown in Figures 8 through 11. A summary of the attenuation values is presented in Table IV-3.

Figure 12 shows a plot of the attenuation vs frequency. The line indicates the slope of any line having a dependence of attenuation on the first power of frequency. All data fall within the limits of data collected by Hamilton [Ref. 14].

3. Reflection Coefficients and Signal Level

Normal incidence pressure reflection and transmission coefficients were measured as an accuracy check on the measured ρ and c values, and also to provide an estimate of the sound pressure level that would be transmitted from the wedge to the underlying medium. A summary of the measured data is presented in Appendix C.

The reflection coefficient R is calculated from

$$R = \frac{|\rho_w c_w - \rho_s c_s|}{|\rho_w c_w + \rho_s c_s|} \qquad (13)$$

and the transmission coefficient T from

$$T = 1 - R \qquad (14)$$

With $\rho_w = 1.00$ g/cm^3, $\rho_s = 1.98$ g/cm^3, $c_w = 1469$ m/s, and $c_s = 1613$ m/s, R is calculated to be 0.37 and T to be 0.63. The measured values of reflection were 0.31 and 0.29. The measured transmission coefficient was 0.65. These values indicate that the measured density and sound speed values are within the expected range.

32
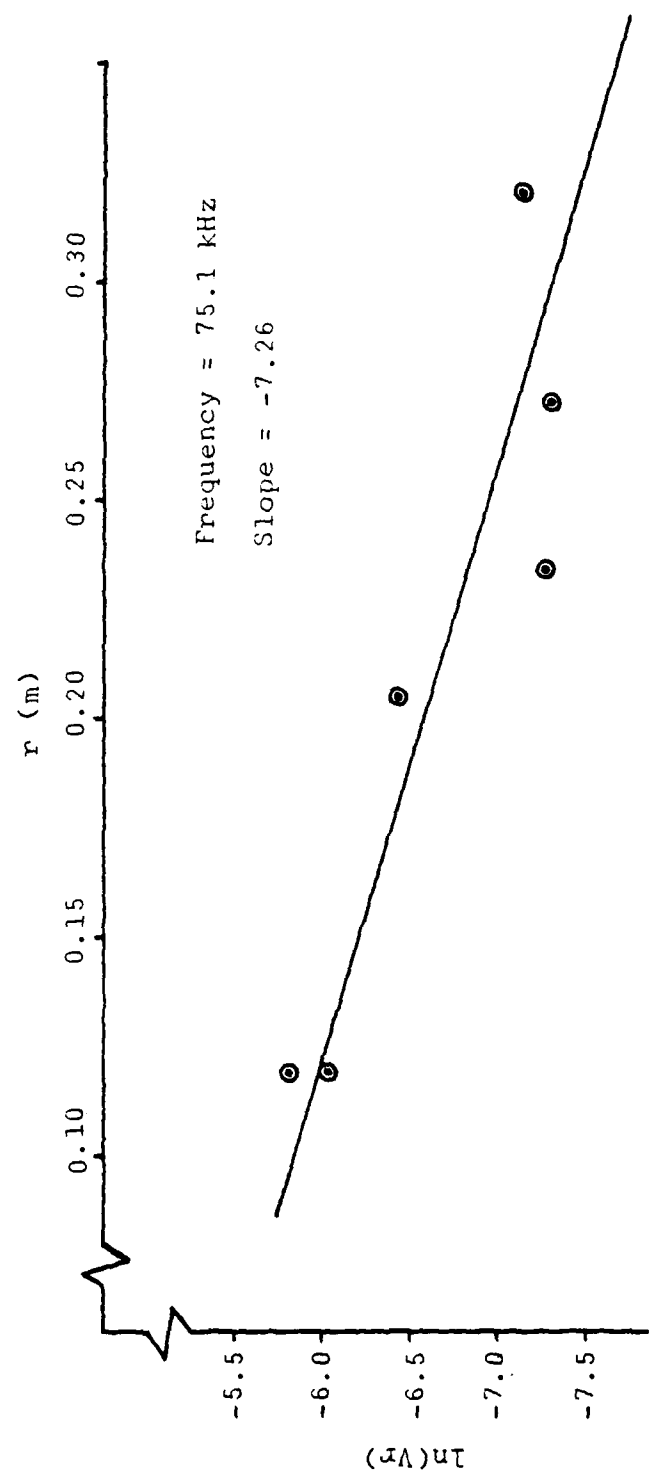
Figure 8.   Attenuation in Sand

33
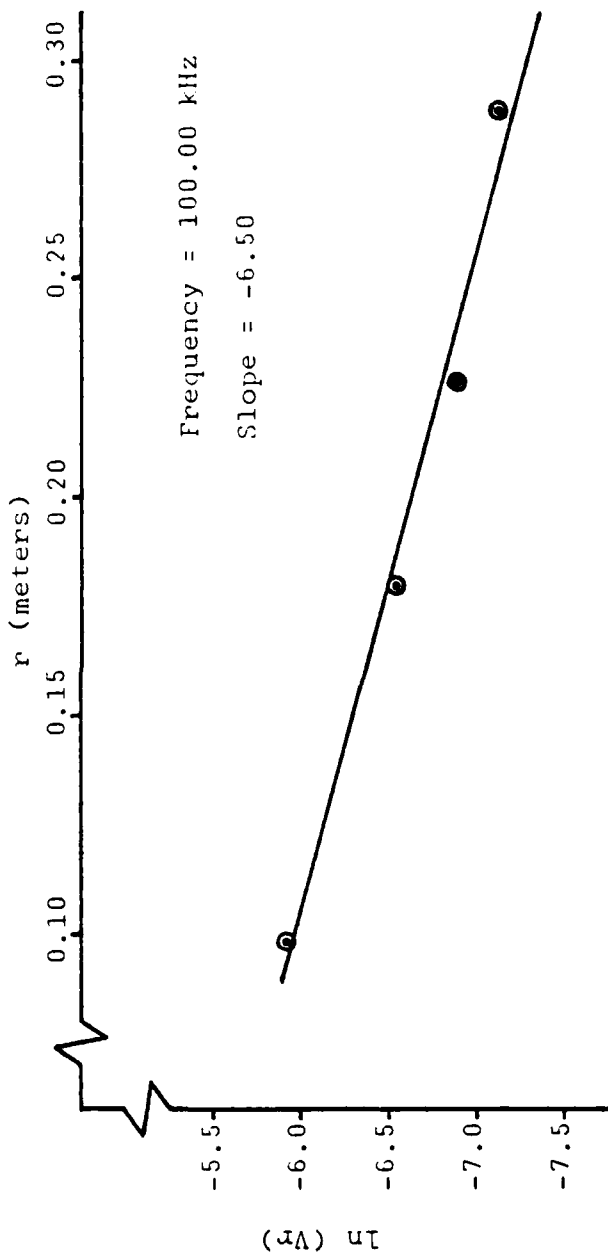
Figure 9. Attenuation in Sand
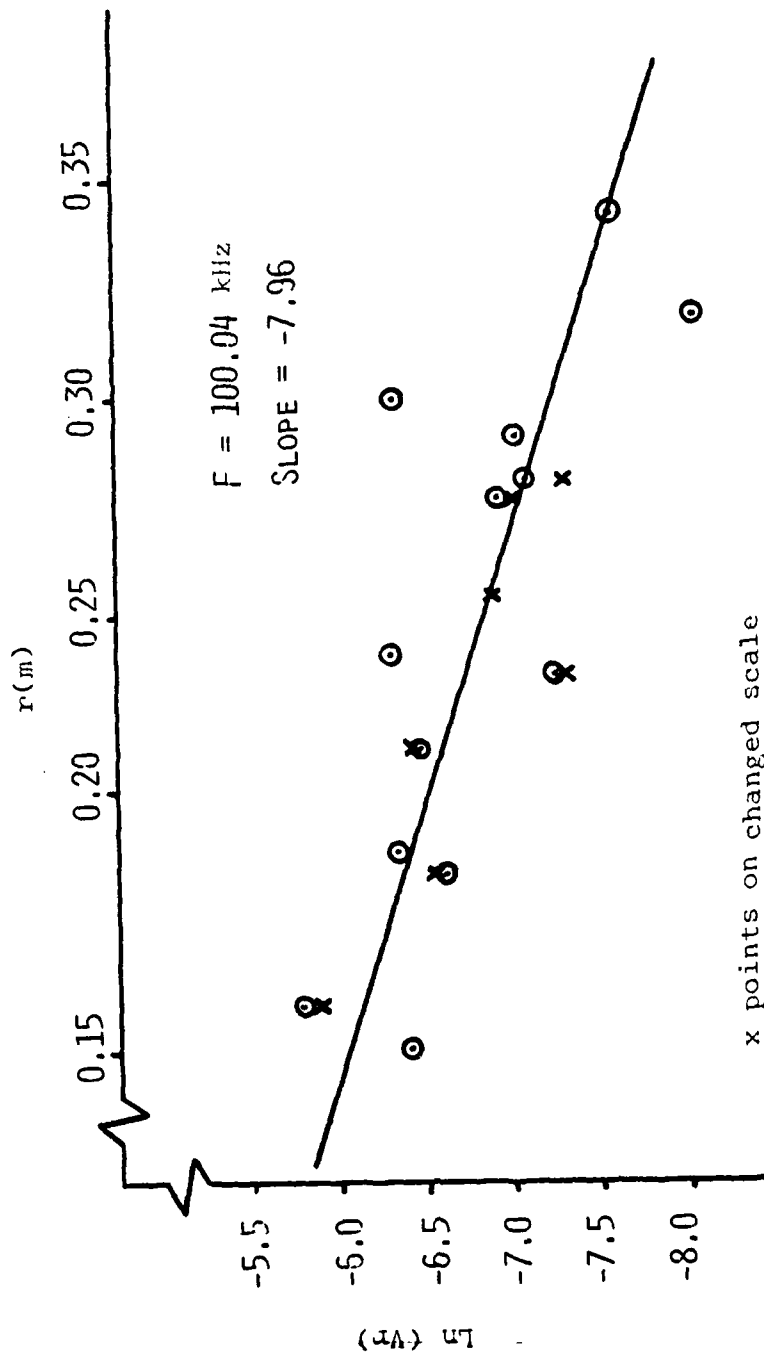
Figure 10. Attenuation in Sand

x points on changed scale

F = 100.04 kHz

SLOPE = -7.96

r(m)

Ln (Vr)

35

Frequency = 130.00 kHz

Slope = − 9.79

r (meters)

Ln (Vr)
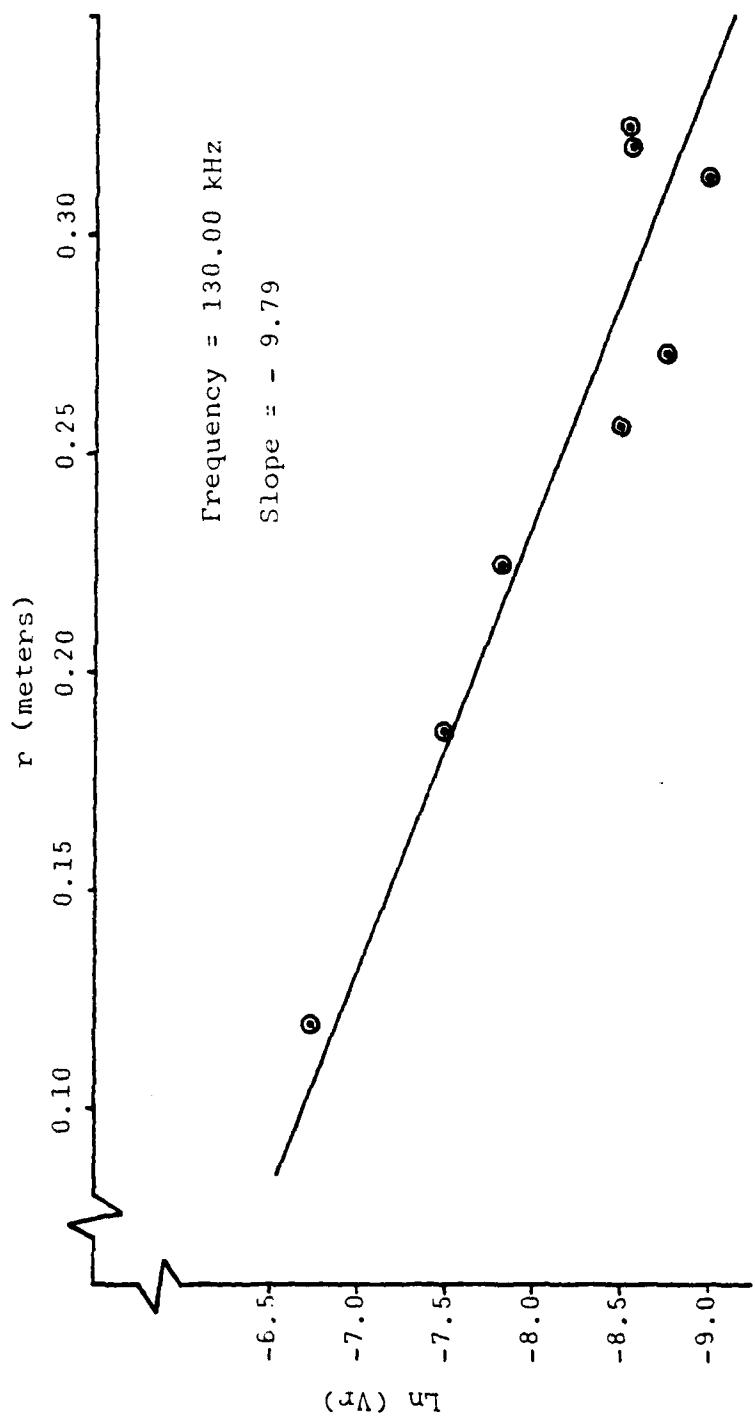
Figure 11. Attenuation in Sand

36
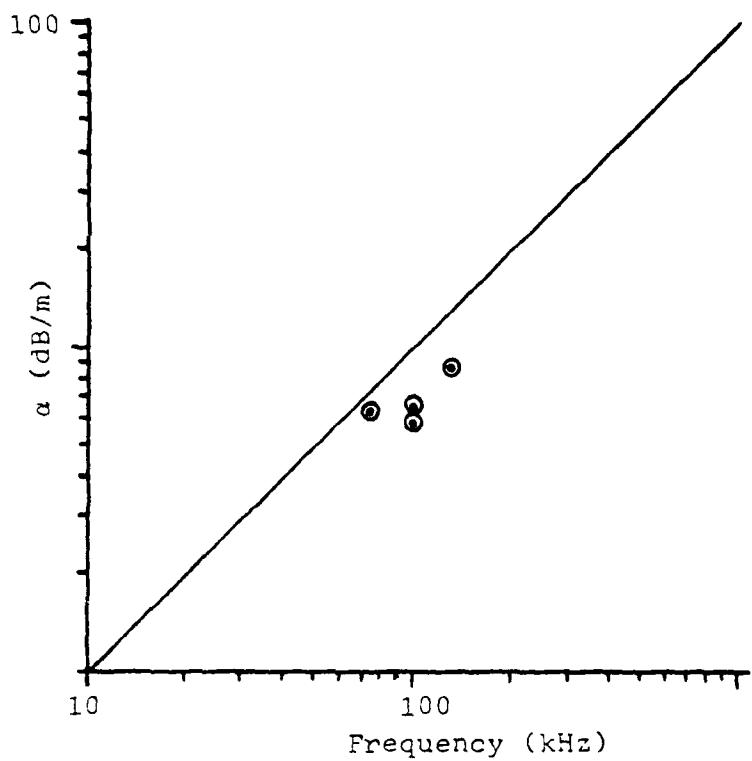
Figure 12. Attenuation vs Frequency

From Table 1 of Appendix C, a received voltage of 6 volts is typical. Assuming a desired reading on the order of 1 volt for test runs, a drop in level of no more than 15.6 dB is indicated. At 100 kHz, the measured attenuation of 56.6 dB per meter would indicate measurements could be made at least 27 cm from the wedge boundary. This satisfies the limit imposed on $\vec{r}$ in Section IV-C-1.

TABLE IV-3. Attenuation Results

f(kHz)	α(Ne/m)	α(dB/m)	Correlation Coefficient
75.10	7.26	63.2	-0.90
100.00	6.50	66.6	-0.99
100.04	7.39	64.3	-0.76
130.00	9.79	85.2	-0.92

V. ERROR ANALYSIS

It is important to know if the physical properties were determined
with sufficient accuracy to verify Bradshaw's model. Bradshaw developed
an analytical equation for the depression angle of the beam formed in
the substrate. As this analytical equation was based on model results,
and since the equation is dependent on all measured physical properties,
the equation should provide a realistic basis for error analysis. The
analytical equation is

$$\theta_D = 17.22 \; \beta^{0.329} \; \theta_c^{0.772} \; (\rho_w/\rho_s)^{-0.254} \tag{15}$$

where θ_D is the beam depression angle in degrees,

β is the wedge angle in degrees,

θ_c is the critical angle in radians,

and ρ_w/ρ_s is the ratio of the density of water to the density of
saturated sand.

The critical angle is defined by

$$\theta_c = \arccos \; (c_w/c_s) \tag{16}$$

where c_w and c_s are the sound speeds in water and sand, respectively.

Using standard error analysis, and noting $\rho_w/\rho_s = 1/\rho_s$,

$$d\theta_D(\beta,\theta_c,\rho_s) = \frac{\delta\theta_D}{\delta\beta} \; d\beta + \frac{\delta\theta_D}{\delta\theta_c} \; d\theta_c + \frac{\delta\theta_D}{\delta\rho} \; d\rho \tag{17}$$

$$= 5.66 \; \theta_c^{0.772} \; (1/\rho_s)^{-0.254} \beta^{0.671} d\beta$$

$$+ 13.29\beta^{0.329} \; (1/\rho_s)^{-0.254} \theta_c^{0.228} d\theta_c$$

$$+ 4.37\beta^{0.329} \theta_c^{0.772} \rho_s^{0.746} d\rho_s$$

Similarly

$$d\theta_c = \frac{\delta\theta_c}{\delta c_w} dc_w + \frac{\delta\theta_c}{\delta c_s} dc_s \qquad (18)$$

$$= \left[\frac{c_w}{c_s^2} dc_s - \frac{1}{c_s} dc_w\right]\left[1 - (c_w/c_s)^2\right]^{-1/2}$$

where $c_w = 1469\pm15$ m/s from Table 2. An error of 3 percent, in keeping with the worst case predicted accuracy from Reference 10, was assigned to sound speed in saturated sand. Therefore, $c_s = 1613\pm48$ m/s and $d\theta_c = 0.04$ radians.

Assuming the wedge angle can be measured to within 0.5 degrees, the following values were used to evaluate equation 17.

$$\rho_s = 1.98 \text{ g/cm}^3 \qquad\qquad d\rho_s = 0.03 \text{ g/cm}^3$$
$$\beta = 3^\circ \qquad\qquad\qquad d\beta = 0.5^\circ$$
$$\theta_c = 0.4257 \text{ rad} \qquad\qquad d\theta_c = 0.04 \text{ rad}$$

Therefore

$$d\theta_D = 3.64 + 0.75 + 0.16$$

$$= 4.55^\circ$$

θ_D for the above parameters is 15.21 degrees. The deviation of 0.75° attributable to sound speed measurements is roughly 5 percent, but is dwarfed by the 3.64° (24 percent) error attributable to the wedge angle measurement. A method of accurately measuring and controlling the wedge angle will be a necessity for successful model test runs.

VI. CONCLUSIONS AND RECOMMENDATIONS

A laboratory sized experiment to test the predictions of Bradshaw's model is possible, using off-the-shelf equipment in a water-over-sand system. Measurements can be made of all necessary physical parameters, and attenuation is not so severe as to preclude measurements at sufficient distances to satisfy model constraints.

Densities and sound speeds were obtained that agreed with literature or theoretical values. The densities of water and saturated sand were 1.00 g/cm^3 and 1.98 g/cm^3, respectively. The sound speed in water was 1469 m/s; the sound speed in saturated sand was 1613 m/s.

The use of a rigid array of receivers is highly recommended for all measurements within the sand in order to control source-receiver spacing.

Model results are strongly dependent on the wedge angle. The sand will maintain a flat, sloped surface, but great care in the formation and measurement of the wedge angle will be required.

It was found necessary to maintain a high bleach concentration in order to control gas producing biologic growth. Every change of water should be accompanied by a renewal of the bleach level.

APPENDIX A

SOUND SPEED IN WATER - DATA

TABLE 1. Two Receivers Direct Path Data

Source Transducer = Homemade Mylar

Separation (cm)	Time (10^{-5} sec)	Sound Speed (meters/second)
6.8	4.50	1511
11.7	7.95	1472
16.7	11.70	1427
19.0	13.30	1428
21.4	14.90	1436
26.3	18.10	1453

$\widetilde{c}$ = 1454 meters/second

σ = 32.6 (2.2%)

TABLE 2. Reflected Path, Varied Distance - Data

Source Transducer = Homemade Mylar

Separation (cm)	Time (10^{-5} sec)	Sound Speed (meters/second)
28.8	19.55	1473
38.8	26.32	1474
48.8	33.25	1468
58.8	40.15	1464
68.8	47.85	1438
78.8	53.70	1467
88.8	59.60	1490
98.8	67.00	1475

$\overline{c}$ = 1469 meters/second

σ = 14.7 (1.0%)

TABLE 3. Reflected Path, Fixed Distance - Data

Source Transducer = LC10 #2338

Separation (cm)	Time (10^{-5} sec)	Sound Speed (meters/second)
22.0	14.92	1474
22.0	15.32	1436
22.0	14.88	1478
22.0	14.92	1474
22.0	14.92	1474
22.0	14.92	1474
22.0	15.32	1436
22.0	15.32	1436
22.0	15.08	1459

$\bar{c}$ = 1460 meters/second

σ = 18.8 (1.3%)

APPENDIX B
SOUND SPEED AND ATTENUATION IN SAND - DATA

TABLE 1. Sound Speed and Attenuation in Sand

Source Transducer = Homemade Mylar
Frequency = 100.04 kHz
Source placed 10 cm below sand surface.

Distance (cm)	Time (10^{-5} sec)	Amplitude (mV)	Sound Speed (meters/second)
15.15	9.04	11.0	1676
16.15	10.10	19.0 (18.0)*	1599
19.15	12.25	7.0 (7.2)	1563
19.60	12.25	9.0	1600
22.05	13.80	7.0 (7.2)	1598
23.75	15.40	3.0 (2.8)	1542
24.10	17.55	7.5	1373**
25.55	15.95	4.0 (4.0)	1602
27.65	17.00	3.5 (3.2)	1626
28.15	19.15	3.0 (2.4)	1470
29.10	18.05	3.0	1612
29.70	18.10	6.0	1641
31.90	20.20	1.0	1579
31.90	21.25	1.5	1501
34.20	22.85	1.5	1497
38.00	no signal	---	----

*changed scale

**omitted point
(outside 2σ)

$\bar{c}$ = 1579 meters/second

σ = 58.6 (3.7%)

46

TABLE 2. Sound Speed and Attenuation in Sand

Source Transducer = Homemade Mylar

Frequency = 100.00 kHz

Source placed 14.5 cm below surface of sand.

Distance (cm)	Time (10^{-5} sec)	Amplitude (mV)	Sound Speed (meters/second)
10.30	6.38	27.0	1614
18.39	11.60	10.0	1585
19.15	12.12	42.0*	1580
23.71	14.26	4.5	1663
29.22	18.94	2.8	1543

*point omitted
 for attenuation

$\bar{c}$ = 1597 meters/second

σ = 44.7 (2.8%)

TABLE 3. Sound Speed and Attenuation in Sand

Source Transducer = Homemade Ceramic

Frequency = 75.1 kHz

Source placed 13.0 cm below sand surface.

Distance (cm)	Time (10^{-5} sec)	Amplitude (mV)	Sound Speed (meters/second)
12.2	9.05	25.0	1348
12.5	8.00	20.0	1562
23.5	16.50	8.0	1424
20.6	14.35	3.0	1436
27.4	19.70	2.5	1391
32.3	22.35	2.5	1445

$$\bar{c} = 1434 \text{ meters/second}$$

$$\sigma = 71.9 \ (5.0\%)$$

TABLE 4.   Sound Speed and Attenuation in Sand

Source Transducer = Homemade Mylar

Frequency = 130.00 kHz

Source placed 7.5 cm below sand surface.

Distance (cm)	Time (10^{-5} sec)	Amplitude (mV)	Sound Speed (meters/second)
12.0	7.7	10.0	1558
13.0	8.0	----	1625
18.7	12.0	3.0	1565
23.0	14.9	1.8	1544
26.1	16.5	0.8	1582
27.3	18.1	0.6	1508
31.5	20.2	0.6	1559
32.2	20.2	0.6	1594
32.6	20.8	0.4	1571

$$\bar{c} = 1567 \text{ meters/second}$$

$$\sigma = 32.6 \ (2.1\%)$$

TABLE 5.   Sound Speed Gradient Data

Source Transducer = LC10 #2338

Frequency = 120.05 kHz

Source and receiver fixed at 30.0 cm separation.

Water (cm)	Sand (cm)	Time (10^{-5} sec)	Amplitude (V)	Sound Speed (meters/second)
11.0	----	20.2	5.4	1485
27.0	----	20.2	10.4	1485
30.0	0.0	18.6	0.5	1613
29.0	1.0	18.6	1.0	1613
27.0	3.0	18.6	2.5	1613
25.5	4.5	18.6	1.35	1613
24.0	6.0	18.6	1.35	1613
23.0	7.0	18.6	1.35	1613
21.0	9.0	18.6	1.35	1613
20.0	10.0	18.6	1.35	1613
17.5	12.5	18.6	1.35	1613
15.0	15.0	18.6	1.35	1613
12.5	17.5	18.6	1.35	1613
10.0	20.0	18.6	1.35	1613

50

APPENDIX C

REFLECTION AND TRANSMISSION COEFFICIENTS - DATA

TABLE 1. Surface Reflection Coefficient

Direct Path		Reflected Path		Reflection Coeff.
Distance (cm)	Amp. (V)	Distance (cm)	Amp. (V)	
22.5	5.8	48.5	2.9	1.077
30.0	5.4	37.2	4.0	0.9185
20.0	6.2	40.0	3.3*	1.010
20.0	6.4	40.0	3.0**	0.9880

$$\overline{R} = 0.998$$

$$\sigma = 0.06$$

* Directivity (.241/.254)

** Directivity (.254/.241)

* and ** measured at normal incidence

TABLE 2. Bottom Reflection Coefficient, Normal Incidence

Distance		Directivity Index
Direct = 20.0 cm		Direct = 0.254
Reflected = 40.0 cm		Reflected = 0.241

Amplitude (V)		Reflection Coefficient
Direct	Reflected	
5.4	0.8	0.31
5.7	0.8	0.30
6.5	0.8	0.26
7.2	1.0	0.29
7.1	1.0	0.30
7.1	0.9	0.27
7.0	1.0	0.30
7.0	0.9	0.27
7.2	1.2	0.35
10.0	1.2	0.25
8.6	1.1	0.27

$$\overline{R} = 0.29$$

$$\sigma = 0.028$$

TABLE 3. Bottom Reflection Coefficient, Normal Incidence

Distance		Directivity Index
Direct = 19.2 cm		Direct = 0.254
Reflected = 40.4 cm		Reflected = 0.241

Amplitude (V)		Reflection Coefficient	
Direct	Reflected		
7.2	1.1	0.34	
7.0	1.2	0.38	
7.5	1.25	0.37	
7.0	1.2	0.38	
7.1	1.0	0.31	
7.6	1.0	0.29	$\overline{R} = 0.31$
7.6	1.0	0.29	$\sigma = 0.044$
7.5	0.8	0.23	
6.5	0.8	0.27	
5.6	0.8	0.32	
6.6	0.9	0.30	
7.4	0.8	0.24	
7.4	0.95	0.28	
7.5	1.0	0.30	
7.0	1.0	0.32	
7.0	1.1	0.35	
7.5	1.2	0.35	
7.0	1.1	0.35	
7.0	0.9	0.29	

TABLE 4. Transmission Coefficient, Normal Incidence

Direct Path = 20.0 cm in water
Transmitted = 10.0 cm in water, 10.0 cm in sand

| Frequency | Amplitude (volts) | | Transmission |
(kHz)	Direct	Transmitted	Coefficient
125	8.7	6.8	0.78
130	9.0	7.0	0.78
125	8.7	5.0	0.57
120	7.8	5.0	0.68
115	7.4	3.6	0.49
110	6.9	3.6	0.52
120	7.8	5.4	0.69
125	8.7	5.2	0.60
130	9.0	7.6	0.84
125	8.7	5.2	0.60
120	7.8	5.2	0.67
115	7.4	3.8	0.51
115	7.4	3.8	0.51
120	7.8	5.2	0.67
125	8.7	5.3	0.61
130	9.0	7.6	0.84

$$\overline{T} = 0.65$$

$$\sigma = 0.116$$

54

LIST OF REFERENCES

1. Tien, P. K., and Martin, R. J., "Experiments on Light Waves in a Thin Tapered Film and a New Light-Wave Coupler", _Applied Physics Letters_, v. 18, p. 398-401, 1 May 71.

2. Kuznetzov, V. K., "Emergence of Normal Modes Propagating in a Wedge on a Half-Space from the Former into the Latter", _Soviet Physical Acoustics_, v. 19, p. 241-245, Nov.-Dec. 1973.

3. Tien, P. K., Smolinsky, G., and Martin, R. J., "Radiation Fields of a Tapered Film and a Novel Film-to-Fiber Coupler", _Transactions on Microwave Theory and Techniques_, v. MTT-23, p. 79-85, January 1975.

4. Sigelman, R. A., et al., "Ocean-Earth Acoustic Coupling", University of Washington Technical Report 209, May 1978.

5. Bradshaw, N. A., _Propagation of Sound in a Fast Bottom Underlying a Wedge-Shaped Medium_, M. S. Thesis, Naval Postgraduate School, Monterey, CA, 1980.

6. Kawamura, M. and Ioannou, I., _Pressure on the Interface Between a Converging Fluid Wedge and a Fast Bottom_, M. S. Thesis, Naval Postgraduate School, Monterey, CA, 1978.

7. Netzorg, G. B., _Sound Transmission From a Tapered Fluid Layer into a Fast Bottom_, M. S. Thesis, Naval Postgraduate School, Monterey, CA, 1977.

8. Kinsler, L. E., and Frey, A. R., _Fundamentals of Acoustics_, p. 118, Wiley & Sons, Inc., 1962.

9. Hamilton, E. L., "Sound Velocity, Elasticity, and Related Properties of Marine Sediments, North Pacific", Naval Undersea Research and Development Center Technical Publication No. 143, v. 1, p. 9-13, October 1969.

10. Anderson, O. L., and Liebermann, R. C., "Sound Velocities in Rocks and Minerals", in _Physical Acoustics_, IV-B, edited by W. P. Mason, Academic Press, 1968.

11. Lange, N. A., _Handbook of Chemistry_, p1199, McGraw-Hill Book Company, 1967.

12. Urick, R. J., _Sound Propagation in the Sea_, Defense Advanced Research Projects Agency, p. 10-14, 1979.

13. Hamilton, E. L., "Sound Velocity Gradients in Marine Sediments",
    J. Acoust. Soc. Am., v. 65, No. 4, p. 909-925, 1979.

14. Hamilton, E. L., "Sound Attenuation as a Function of Depth in the
    Sea Floor", J. Acoust. Soc. Am., v. 59, No. 3, p. 528-535, 1976.

INITIAL DISTRIBUTION LIST

		No. Copies
1.	Defense Technical Information Center Cameron Station Alexandria, VA 22314	2
2.	Library, Code 0142 Naval Postgraduate School Monterey, CA 93940	2
3.	Chairman (Code 68Mr) Department of Oceanography Naval Postgraduate School Monterey, CA 93940	1
4.	Chairman (Code 63Rd) Department of Meteorology Naval Postgraduate School Monterey, CA 93940	1
5.	Department Library, Code 61 Department of Physics and Chemistry Naval Postgraduate School Monterey, CA 93940	2
6.	Department Chairman, Code 61 Department of Physics and Chemistry Naval Postgraduate School Monterey, CA 93940	1
7.	Dr. J. V. Sanders, Code 61Sd Department of Physics and Chemistry Naval Postgraduate School Monterey, CA 93940	5
8.	Dr. R. H. Bourke, Code 68Bf Department of Oceanography Naval Postgraduate School Monterey, CA 93940	1
9.	Dr. A. B. Coppens, Code 61Cz Department of Physics and Chemistry Naval Postgraduate School Monterey, CA 93940	1

10. LT James A. Bradshaw   1
    99 Corona Rd.
    Carmel, CA 93923

11. Chief of Naval Research
    Department of the Navy
    800 North Quincy Street
    Arlington, Virginia 22217
      Code 100C1   1
      Code 460   1
      Code 463   5
      Code 464   1
      Code 480   1

12. Commanding Officer   1
    Office of Naval Research Branch Office
    1030 East Green Street
    Pasadena, CA 91106

13. Director   6
    Naval Research Laboratory
    Code 2627
    Washington, D.C. 20375

14. Office of Research, Development,   1
    Test, and Evaluation
    Department of the Navy
    Code NOP-987J
    Washington, D.C. 20350

15. Director   1
    Defense Advanced Research
    Projects Agency
    1400 Wilson Boulevard
    Arlington, Virginia 22209

16. Air Force Office of Scientific Research   1
    Department of the Air Force
    Directorate of Physics (MPG)
    Building 410
    Bolling Air Force Base
    Washington, D.C. 20332

17. Army Research Office   1
    Department of the Army
    Geoscience Division
    Box 12211
    Research Triangle Park, North Carolina 27709

18. Director   1
    Naval Oceanography Division
    Naval Observatory
    34th and Massachusetts Avenue NW
    Washington, D.C. 20390

19. Commander   1
    Naval Oceanography Command
    NSTL Station
    Bay St. Louis, MS 39522

20. Commanding Officer   1
    Naval Oceanographic Office
    NSTL Station
    Bay St. Louis, MS 39522

21. Commanding Officer   1
    Fleet Numerical Oceanography Center
    Monterey, CA 93940

22. Commanding Officer   1
    Naval Ocean Research and Development Activity
    NSTL Station
    Bay St. Louis, MS 39522

23. Commanding Officer   1
    Naval Environmental Prediction Research Facility
    Montery, CA 93940

24. Chairman, Oceanography Department   1
    U.S. Naval Academy
    Annapolis, MD 21402

25. Office of Naval Research (Code 480)   1
    Naval Ocean Research and Development Activity
    NSTL Station
    Bay St. Louis, MS 39522

26. Scientific Liaison Office   1
    Office of Naval Research
    Scripps Institution of Oceanography
    La Jolla, CA 92037

27. Library   1
    Scripps Institution of Oceanography
    P.O. Box 2367
    La Jolla, CA 92037

28. Library   1
    Department of Oceanography
    University of Washington
    Seattle, WA 98105

29. Library   1
    CICESE
    P.O. Box 4803
    San Ysidro, CA 92073

30. Library   1
    School of Oceanography
    Oregon State University
    Corvallis, OR 97331

31. Commander   1
    Oceanographic Systems Pacific
    Box 1390
    Pearl Harbor, HI 96860

32. Dr. W. A. Kuperman   1
    SACLANT ASW Research Centre
    APO New York 09019

33. Dr. David Blackstock   1
    Applied Research Laboratories
    The University of Texas at Austin
    Post Office Box 8029
    Austin, Texas 78712

34. Commander Ioannis Ioannou   1
    Xanthipou-7
    Holargos
    Athens, Greece

35. Lieutenant Masami Kawamura   1
    Ohara Kanshya 1-305
    Etajima
    Hiroshima, Japan